SI APPENDIX

Interplay between tolerance mechanisms to copper and acid stress in *Escherichia coli*

Karrera Y. Djoko*, Minh-Duy Phan, Kate M. Peters, Mark J. Walker, Mark A. Schembri, and Alastair G. McEwan

School of Chemistry and Molecular Biosciences and Australian Infectious Diseases Research Centre, The University of Queensland, St Lucia, QLD 4072, Australia

SI Discussion 1.

Fig. S14 suggested that the amount of Cu required to directly inhibit the activity of mature GOGAT enzyme was higher at pH 5 (10 μM *vs.* 1 μM at pH 7). Earlier, we showed that expression of *gltB* was higher at pH 5 (Fig. 4C(ii)). Similarly, GOGAT activities were higher at pH 5 (Fig. 4D(ii), Figure S10). Therefore, the intracellular concentration of GOGAT enzyme was likely higher in cells cultured at pH 5. Consistently, a higher amount of Cu was required to inhibit GOGAT activity directly at pH 5.

These results seemed to contradict results in Fig. 4D(ii), in which lower amounts of Cu were required to achieve inhibition of GOGAT during growth at pH 5 (0.05 μM *vs.* 0.5 μM at pH 7). However, in these earlier experiments, Cu was added to the culture at the start of the growth and GOGAT activity was measured only when cells reached the mid-exponential phase (after at least 4 generations). The observed loss in GOGAT activity here would be the combined effect of direct enzyme inactivation (as shown in Fig. S14) as well as inhibition of downstream processes that may affect enzyme biogenesis, *eg. via* the Isc pathway for Fe-S cluster assembly (as shown Fig. S12).

SI Discussion 2.

The Δ*copA*Δ*cueR* mutant was found to be reproducibly more Cu-tolerant at pH 7 compared with the Δ*copA* parent strain when growth was assessed in parallel (Fig. S15). The mechanism for the increased tolerance at pH 7 is unknown and is beyond the scope of our work.

At pH 5, the Δ*copA*Δ*cueR* double mutant was reproducibly more Cu-sensitive than was the Δ*copA* parent strain (Fig. S15). On several occasions, growth of the Δ*copA*Δ*cueR* mutant was affected even in the absence of added Cu and background expression levels of *ybaS* and *ybaT* genes were higher than usual. This was likely a consequence of trace Cu in the

culture medium, which varied between 10–20 nM. These basal amounts of Cu approached inhibitory levels and the precise threshold varied with medium preparations.

To determine if Cu stress induced the expression of *ybaS* and *ybaT* in the Δ*copA*Δ*cueR* mutant, we cultured this mutant in the presence of 30 nM Cu. Parallel experimentation with the the Δ*copA* mutant (in the same media preparation, in the presence of 50 nM Cu as usual) as a positive control yielded consistent results and *ybaS* and *ybaT* were reproducibly upregulated during Cu stress (Fig. S16). However, given the challenges described above, it was difficult to obtain reproducible results with the Δ*copA*Δ*cueR* mutant. On the basis that we were able to find three independent replicates where *ybaS* and *ybaT* were upregulated by Cu (Fig. S16), we concluded that CueR does not control *ybaS* and *ybaT* directly under our experimental conditions.

SI Methods

Bioinformatic analyses. The nucleotide sequences of the *copA-ybaST-cueR* locus from *E. coli* K-12 str. MG1655 (6526 bp, RefSeq NC_000913.3) and the *copA-cueR* locus from *S. enterica* subsp. *enterica* sv. Typhimurium str. LT2 (3029 bp, RefSeq NC_003197.1) were used to query all complete genomes on NCBI (5975 available, last accessed 24/11/2016) using MegaBLAST (v.2.4.0+). Results were visualized using ggplot2 (v.2.2.0) in R (v.3.3.1). Distribution of YbaS was determined by tblastn against the same database with a threshold of 60% identity and 80% coverage. Genomic context was illustrated using Easyfig (1) with manual modification using Inkscape (v.0.91).

Measurement of intracellular Glu content. Bacterial pellets from batch cultures (50 mL) were resuspended in MeOH/MeCN/H_2O (40/40/20 v/v/v %) with frequent vortexing and re-centrifuged. The supernatant was evaporated to dryness under vacuum at 40 ^oC and the

resulting pellet was resuspended in water. Insoluble debris were removed by centrifugation and the supernatant was added to a reaction mixture containing hydrazine (250 mM), ADP (1 mM), NAD^+ (1.6 mM), and *L*-glutamic dehydrogenase (Sigma G7882, 160 μg/mL) in Tris-Cl buffer (100 mM, pH 9). The mixture was incubated at 37 ^oC for 30–60 min. Glu concentrations in the samples were estimated by comparing final absorbance values at 340 nm against a standard curve. Glu levels in UTI89 strains cultured at pH 7 and pH 5 were routinely measured to be ~44 and ~9 nmol/mg protein, respectively. A parallel culture in Gutnick medium (2) without any added Cu yielded ~90 nmol Glu/mg protein, suggesting that our culture conditions in modified M9 medium were Glu-limiting, particularly at pH 5.

Measurements of enzyme activities. Centrifuged bacterial pellets from batch cultures (50 mL) were resuspended in 0.5 mL of Na-HEPES buffer (50 mM, pH 7.4) and lysed by sonication (5 × 10 s bursts,10 W each). Each lysate was centrifuged and the supernatant was added into the appropriate reaction mixture in Na-HEPES buffer (50 mM, pH 7.4) as described below. All reactions were performed at 37 ^oC. Amounts of proteins in samples were quantified using QuantiPro^{TM} BCA Assay Kit (Sigma).

GOGAT and GDH activities were determined by following the oxidation of NADPH (0.25 mM). Gln (2.5 mM) and a-KG (2.5 mM) were used as substrates for GOGAT. Absorbance values at 340 nm were monitored continuously for 2 min (1 U = 10 nmol NADPH oxidised/min/μg protein). Gln was replaced with ammonium chloride (25 mM) for GDH (1 U = 1 nmol NADPH oxidised/min/μg protein). The activity of NUO was estimated by following the oxidation of deamino-NADH (Sigma N6756, 0.25 mM) at 340 nm for 2 min (1 U = 1 nmol deamino-NADH oxidised/min/mg protein). SDH activity was determined by monitoring the reduction of thiazolyl blue tetrazolium bromide (MTT, 0.15 mM) at 570 nm for 15 min in the presence of sodium succinate (5 mM) and phenazine methosulfate (PMS,

0.5 mM) (1 U = 1 nmol of MTT reduced/min/mg protein). To estimate the activities of YbaS and YneH, cell-free lysate supernatants were incubated with Gln (50 mM) at 37 ^{o}C for 20 min in MES (100 mM, pH 5.5) and HEPES (100 mM, pH 7.4) buffer, respectively. The mixture was heated to 75 ^{o}C for 5 min to deactivate all enzymes and chilled to 4 ^{o}C. Enzyme activities were estimated from the amount of Glu generated in the reaction (1 U = 1 nmol Glu hydrolysed/min/mg protein).

RNA extraction and measurement of gene transcripts. For RNA extraction, 1 mL of the batch culture was harvested separately by centrifugation (15,000 *g*), snap-frozen, and stored at −80 ^{o}C until further use. Bacterial RNA was extracted using the RNeasy Mini Kit (QIAGEN) and treated with DNAseI using the RNase-Free DNase Set (QIAGEN). cDNA was generated from 0.5 µg of RNA using the SuperScript® III First-Strand Synthesis System (Invitrogen). qPCR analyses were performed in 10 µL reactions using 2 ng of cDNA as template and 0.4 µM of the appropriate primer pairs (Table S2). Each sample was analysed in three technical replicates. Amplicons were detected with SYBR Green 2 in a QuantStudio 6 Flex Real-Time PCR System (Applied Biosystems). C_q values were calculated using LinRegPCR (3) after correcting for amplicon efficiency. *holB*, which encodes for DNA polymerase III, was used as the reference gene as its expression was not affected by metal ions (4).

SI References

1. Sullivan MJ, Petty NK, & Beatson SA (2011) Easyfig: a genome comparison visualizer. *Bioinformatics* 27(7):1009-1010.

2. Bennett BD*, et al.* (2009) Absolute metabolite concentrations and implied enzyme active site occupancy in Escherichia coli. *Nat. Chem. Biol.* 5(8):593-599.

3. Ramakers C, Ruijter JM, Deprez RH, & Moorman AF (2003) Assumption-free analysis of quantitative real-time polymerase chain reaction (PCR) data. *Neurosci. Lett.* 339(1):62-66.

4. Graham AI*, et al.* (2009) Severe zinc depletion of Escherichia coli: roles for high affinity zinc binding by ZinT, zinc transport and zinc-independent proteins. *J Biol Chem* 284(27):18377-18389.

SI TABLES

Table S1. Primers used for making mutant strains. All primers were purchased from Integrated DNA Technologies (Australia). Sequences belonging to the *cat* and *kan* cassettes from pKD3 and pKD4 plasmid, respectively, are in lowercase. Sequences belonging to *E. coli* strain UTI89 (RefSeq NC_007946.1) or EC958 (RefSeq NZ_HG941718.1) are in UPPERCASE. Restriction sites are in **bold**. Ribosomal binding sites are underlined.

Target	Flanking region	Primer Name	Sequence (5' → 3')
Δ*copA*[a]	5'	F	CTTTGTCCTGTACCGCCTGC
		R	ggaataggaactaaggaggaGGTCAGGTCGATAGTTTGTG
	3'	F	cctacacaatcgctcaagacGTGAGTAACGCCAACCGCTT
		R	AAATGGGTTAATGGCAAGGC
Δ*ybaST*	5'	F	CCTCAGAAACCGCTGTCAGT
		R	ggaataggaactaaggaggaTTTGTTTGCATCTAACATCTTTTGT
	3'	F	cctacacaatcgctcaagacATGAAGCGCAATAAAACCGTATAAC
		R	TTTTCGATAATCGGGCAGTC
Δ*copA* Δ*ybaST*	5'	F	AAATGGGTTAATGGCAAGGC
		R	ggaataggaactaaggaggaGTGAGTAACGCCAACCGCTT
	3'	F	cctacacaatcgctcaagacATGAAGCGCAATAAAACCGTATAAC
		R	TTTTCGATAATCGGGCAGTC
Δ*cueR*[b]	5'	F	TCATGGACAACATGGGCAGC
		R	gaagcagctccagcctacacaTCGCTAATGTTCATCGTTCG
	3'	F	ctaaggaggatattcatatgCTCTCCGGCTGCTGTCAT
		R	ACAGCGTCAGACGGCTATTT
pSU2718 -*copA*	-	F	*catgga***GGATCC**ttaaagaggagaaaggtaccgcATGTCACAAACTATCGACCTGAC
		R	*ttacgc***TCTAGA**CGCATCCGCAATGATGTACT
pSU2718 -*ybaST*	-	F	*catgga***GGATCC**ttaaagaggagaaaggtaccgcATGTTAGATGCAAACAAATTACAGC
		R	*ttacg***CTCTAGA**TGTGCTTTGTTAAAGGGTTTCA

[a]These primers were used to generate the Δ*copA* mutant in both UTI89 and EC958 backgrounds.
[b]This mutation was introduced in the UTI89Δ*copA* background to generate UTI89Δ*copA*Δ*cueR* double mutant.

Table S2. Primers used for analyses of gene transcription by qPCR. Primers were purchased from Sigma (Australia). Genome sequence of *E. coli* strain UTI89 (RefSeq NC_007946.1) was used as template.

Amplicon name	Primer sequence (5' → 3')	Amplicon length (bp)
copA	F: ATGACGATGACAGCCAGCAG R: TTTACCCGTGCCTGAGTGAC	112
cueO	F: AACCAGTGAAGGTGAGCGAG R: CATCCCCATCTGACTGACCG	119
cueR	F: GAAGAGAAGGGGCTGGTGAC R: CCTCCAGGTTAAAGCCCACC	124
gltB	F: AAGGTCTGTGTATGCCGACG R: GCGGTACGGTGTTAGTGGAG	114
holB	F: GTGGTGCGAAAGTTGTCTGG R: CGCGGGTAGCAAGGAAAAAC	120
sufA	F: GCTTTGGCTATGTGCTCGAC R: CTTGCAGCGGGACAAACAG	93
sufB	F: TGGAGATGGAAGAACCGCAC R: GTCACAATTACCGCACGATGG	98
ybaS	F: ACCAACTTCCATAACCGGGC R: TTGATGAGCGTGGAGCACTG	113
ybaT	F: TAAGCAACCATGCGGTAGGG R: AGAAACGGAAATATGCGCCG	119

SUPPORTING FIGURES

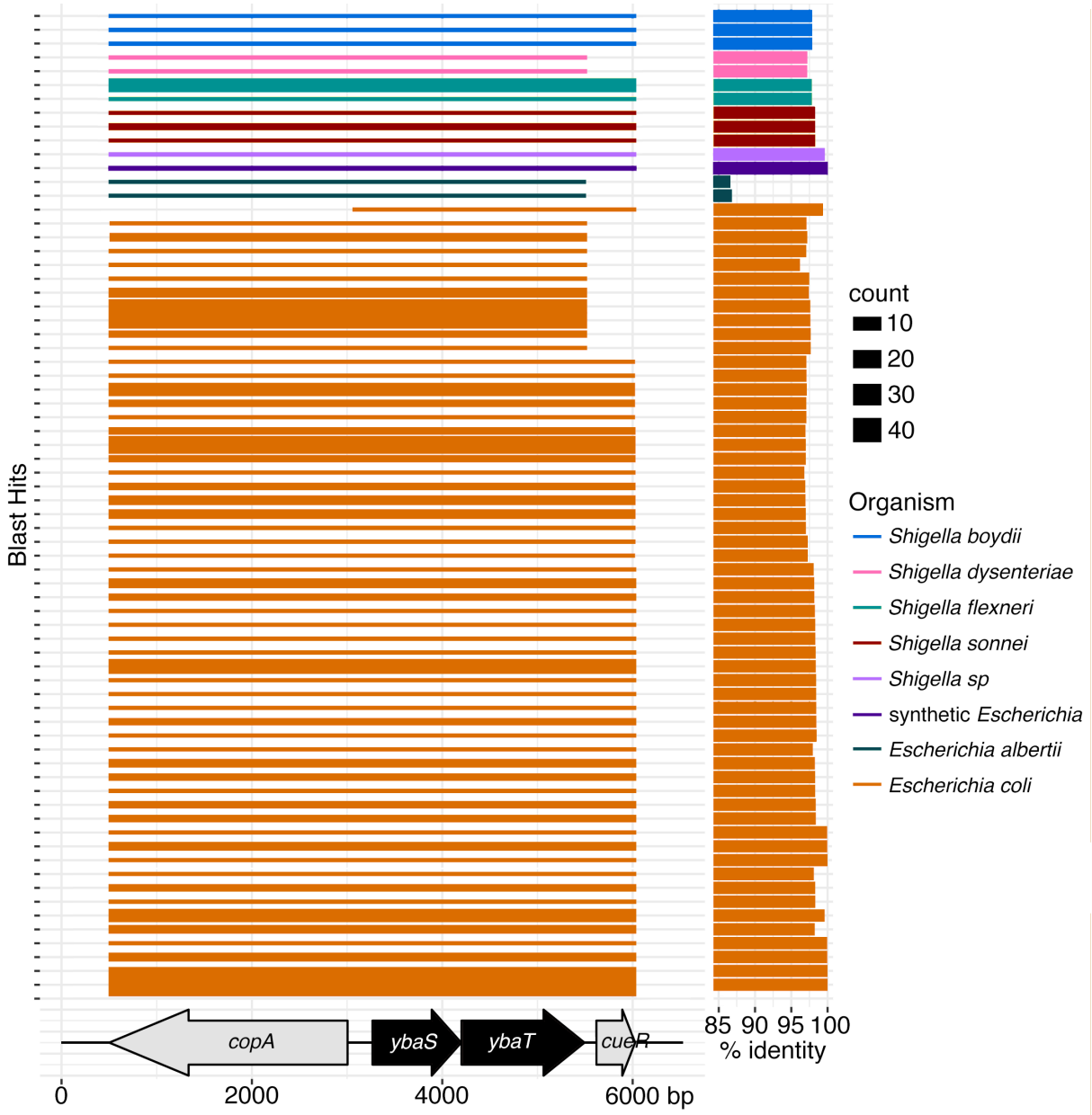

Figure S1. Sequence alignments of *copA-ybaST-cueR* loci. The sequence of the *copA-ybaST-cueR* locus from *E. coli* was used as a query in a BLASTn search against 5975 complete bacterial genomes. The search yielded a total of 232 positive hits with alignment length covering *ybaST*. Each horizontal line represents a unique alignment group belonging to the same species that has the same % identity over the same alignment length. The line thickness represents the number of hits in each group and is coloured according to species name.

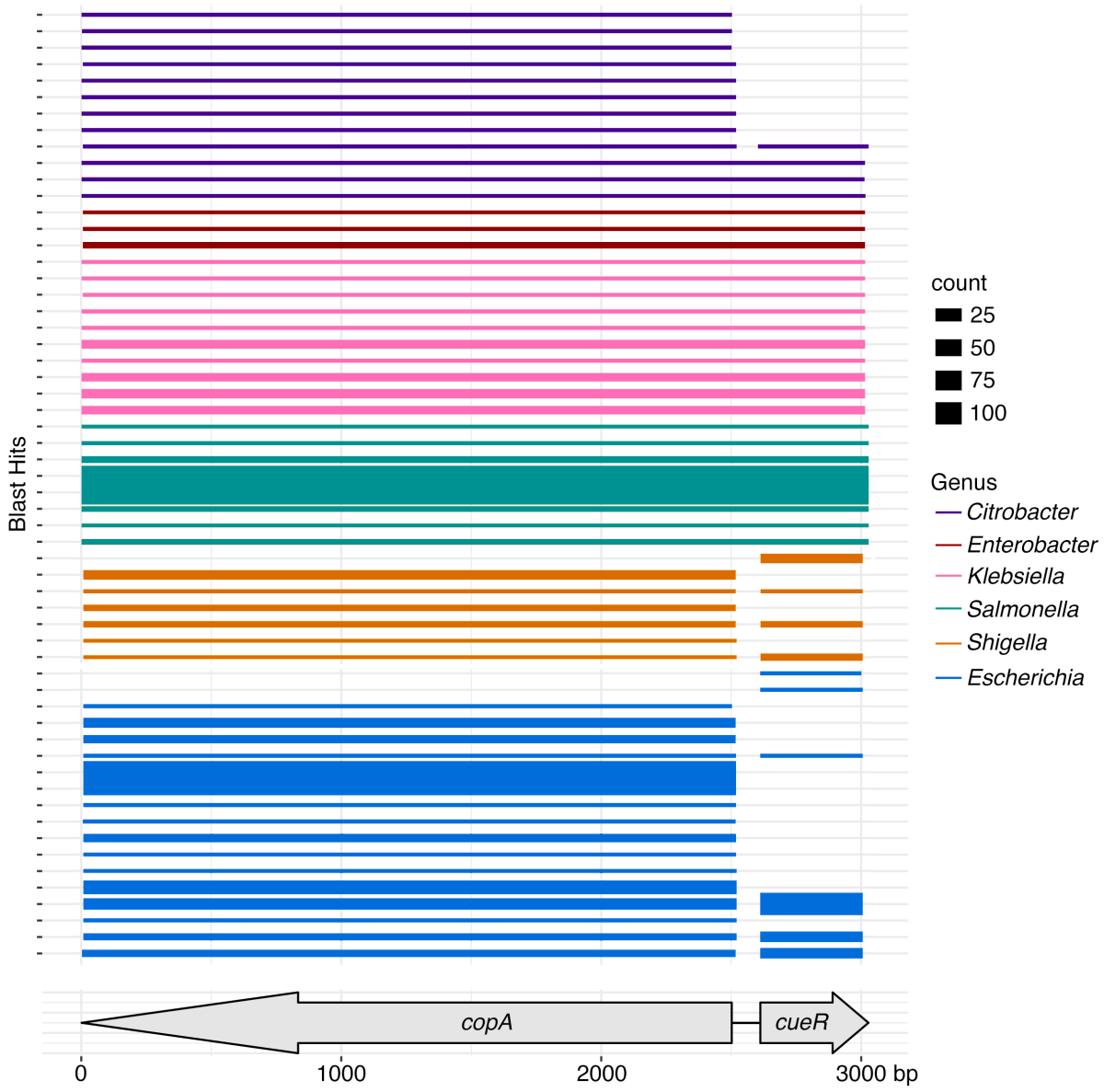

Figure S2. Sequence alignments of *copA-cueR* loci. The sequence of the *copA-cueR* locus from *S. enterica* sv. Typhimurium was used as a query in a BLASTn search against 5975 complete bacterial genomes. The search yielded a total of 262 positive hits with alignment length covering *copA* and *cueR* without *ybaST* insertion, shown by continuous horizontal lines with no gap. Hits from *Escherichia* and *Shigella* genera, which include *ybaST* insertion were also shown by horizontal lines with a gap between *copA* and *cueR* for comparison. Each horizontal line represents a unique alignment group belonging to the same species that has the same % identity over the same alignment length. The line thickness represents the number of hits in each group and is coloured according to species name.

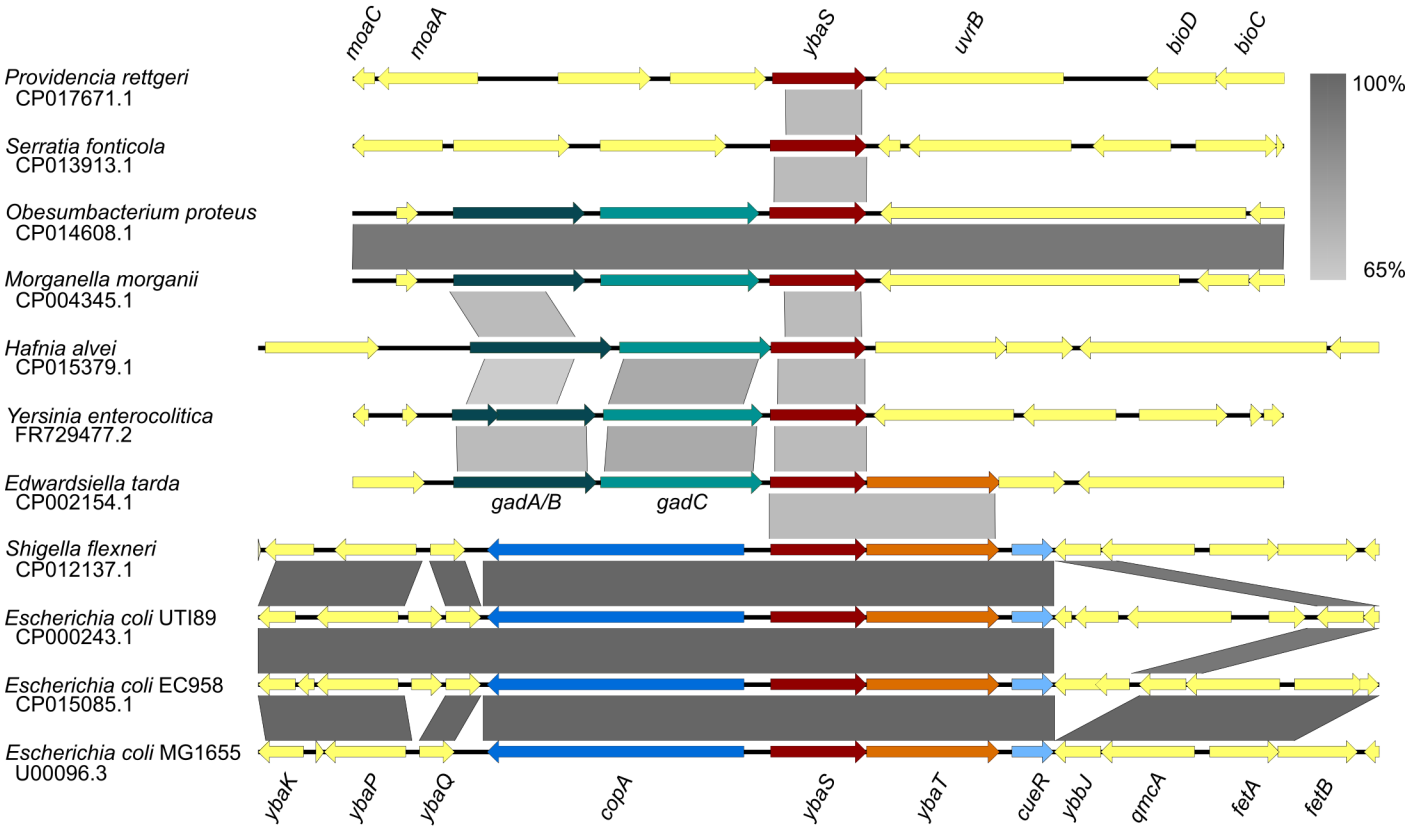

Figure S3. Genomic context of *ybaS* in several *Enterobactericeae* species. The protein sequence of YbaS was used to query 5975 complete bacterial genomes by tblastn. The search identified 325 genomes positive for YbaS (>60% identity over 80% coverage) from 15 genera. One genome per genus from *Enterobacteriaceae* family was chosen to represent the YbaS-encoding locus plus 5 kb flanking regions. The *copA-ybaS-ybaT-cueR* arrangement is confined within *E. coli* and *Shigella* while *ybaS* is located elsewhere in the genomes of other genera.

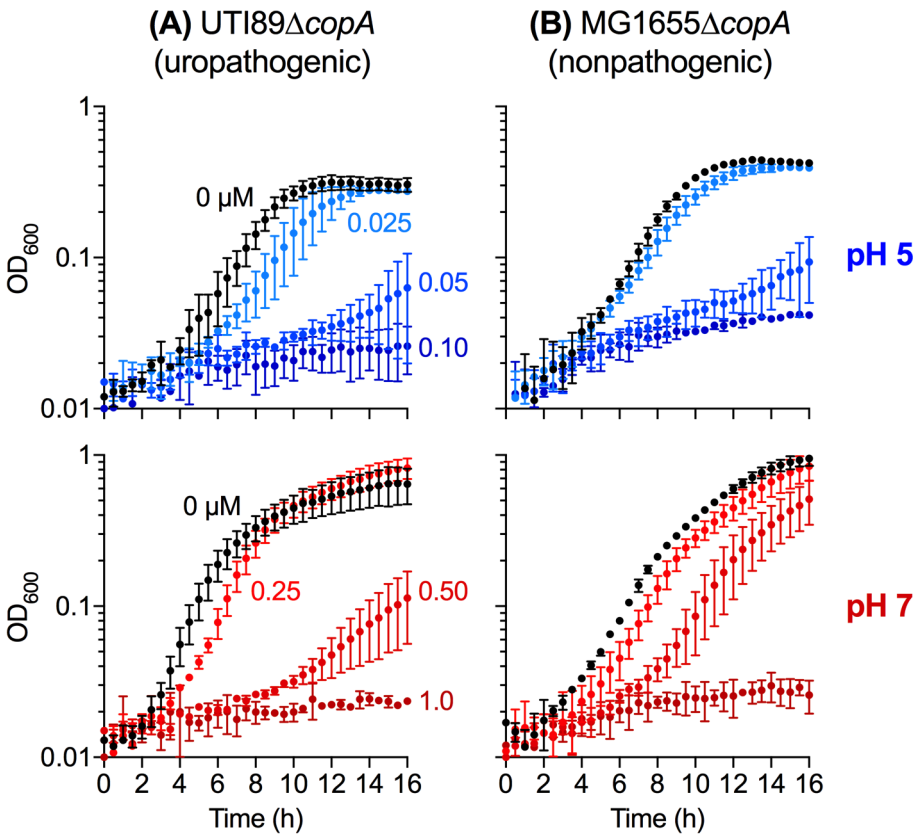

Figure S4. Cu stress in different *E. coli* strains. The Δ*copA* mutant strains of **(A)** UTI89 and **(B)** K-12 substr. MG1655 were cultured at pH 5 and pH 7 in the presence of various concentrations of Cu as indicated. Data were averaged from three independent experiments. Error bars represent ± SD.

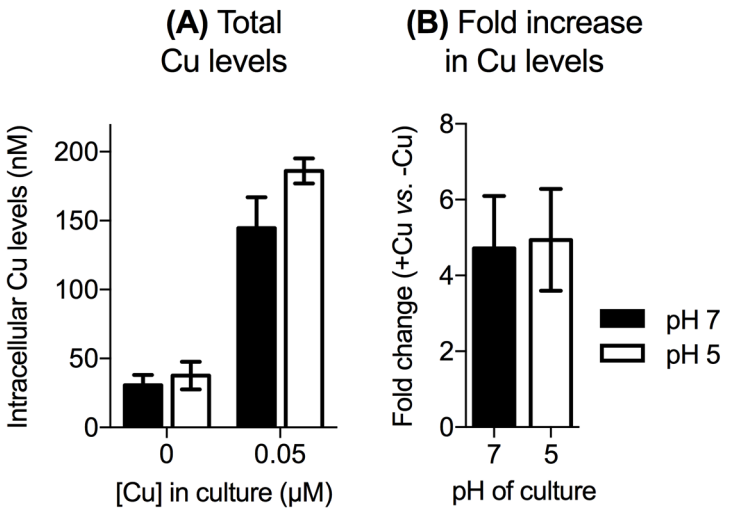

Figure S5. (A) Total amounts of intracellular Cu in UTI89Δ*copA*. Bacteria were cultured at pH 7 (black columns) or pH 5 (white columns) to a final OD_{600} of ~0.3. The medium was supplemented with 0 or 0.05 µM Cu as indicated. Bacteria were centrifuged, washed once with ice-cold PBS containing 1 mM EDTA and twice more with ice-cold PBS without any EDTA. Bacterial pellets were dried overnight at 50 ^{o}C and dissolved in conc. nitric acid (100 µL) with heating at 90 ^{o}C. Each sample was diluted to 10 mL with deionised water and sent for metal analyses using Inductively-Coupled Plasma Mass Spectrometry at the School of Earth Sciences, The University of Queensland. Cu levels were normalised to protein content. Intracellular Cu concentrations (in nM) were calculated using the assumption that the protein concentration inside an *E. coli* cell is ~300 mg/mL. **(B) Fold increase in intracellular Cu levels.** This was calculated using data from panel (A). **(A-B)** Results were averaged from five independent experiments. Error bars represent ± SD.

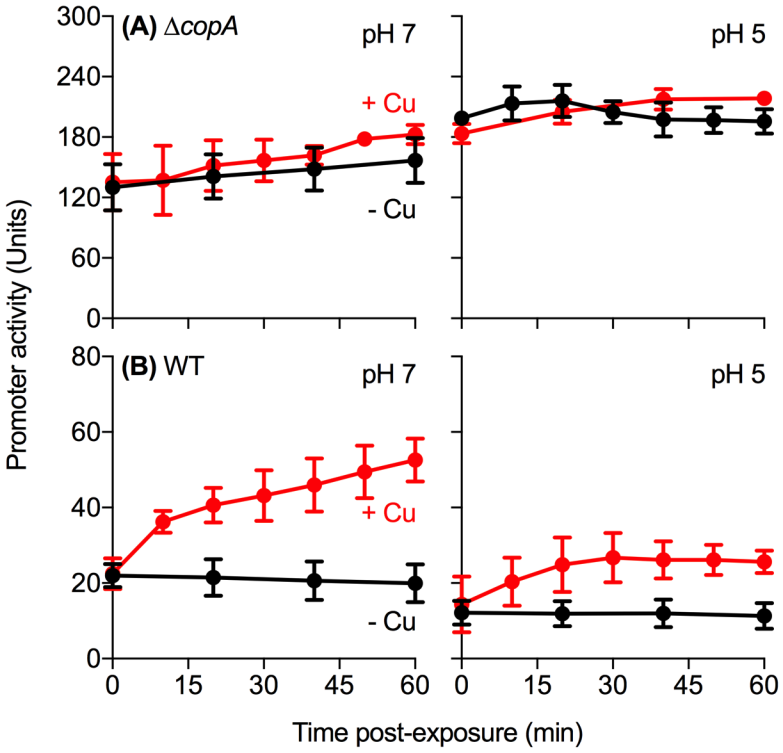

Figure S6. Response of P_{copA}-*lacZ* reporter to Cu stress at pH 7 and pH 5. *E. coli* UTI89 **(A)** Δ*copA* mutant and **(B)** WT strains harbouring the P_{copA}-*lacZ* plasmid were cultured at pH 7 or pH 5 without any added Cu. Upon reaching the mid-exponential phase, bacteria were challenged with water (-Cu, black traces) or 1 µM of added Cu (+Cu, red traces) in the same medium. Bacteria were collected at intervals up to 60 min post-exposure. β-galactosidase activities were measured following standard protocol using *o*-nitrophenyl-β-galactoside (1 mg/mL) as substrate. The total volume of each sample was 200 µL. Absorbance values at 420 nm were recorded in microtitre plates and results were expressed as Miller units. Data were averaged from three independent experiments. Error bars represent ± SD.

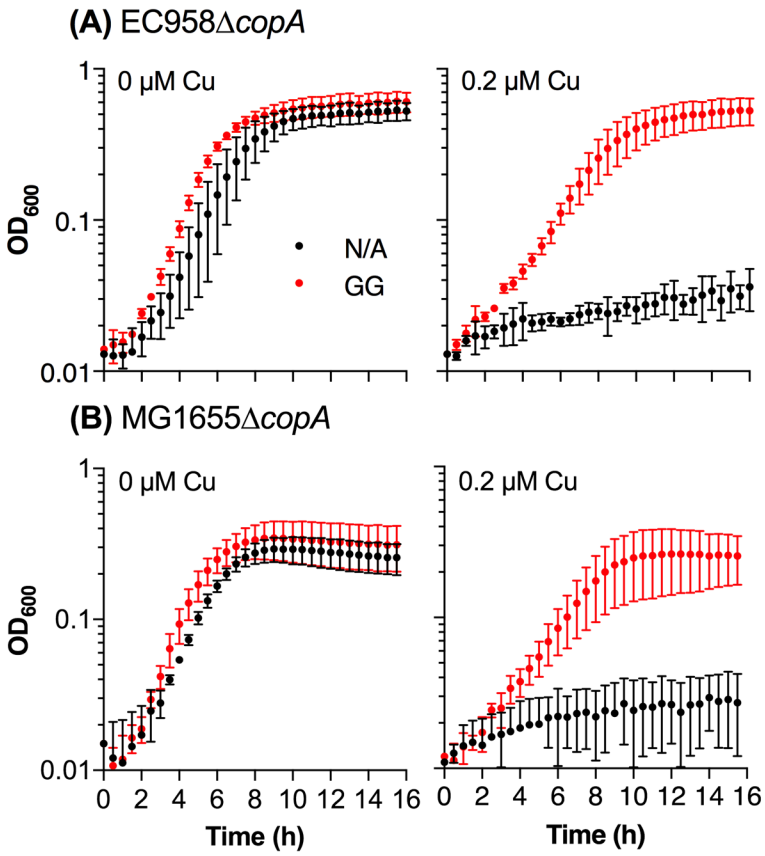

Figure S7. Protective effects of Glu and Gln in different *E. coli* strains. *E. coli* **(A)** EC958Δ*copA* and **(B)** MG1655Δ*copA* mutant strains were cultured at pH 5 in the presence of 0 or 0.2 μM added Cu. The medium was supplemented with water (black, N/A) or a combination of Glu and Gln (0.25 mM each, red, GG). Data were averaged from three independent experiments. Error bars represent ± SD.

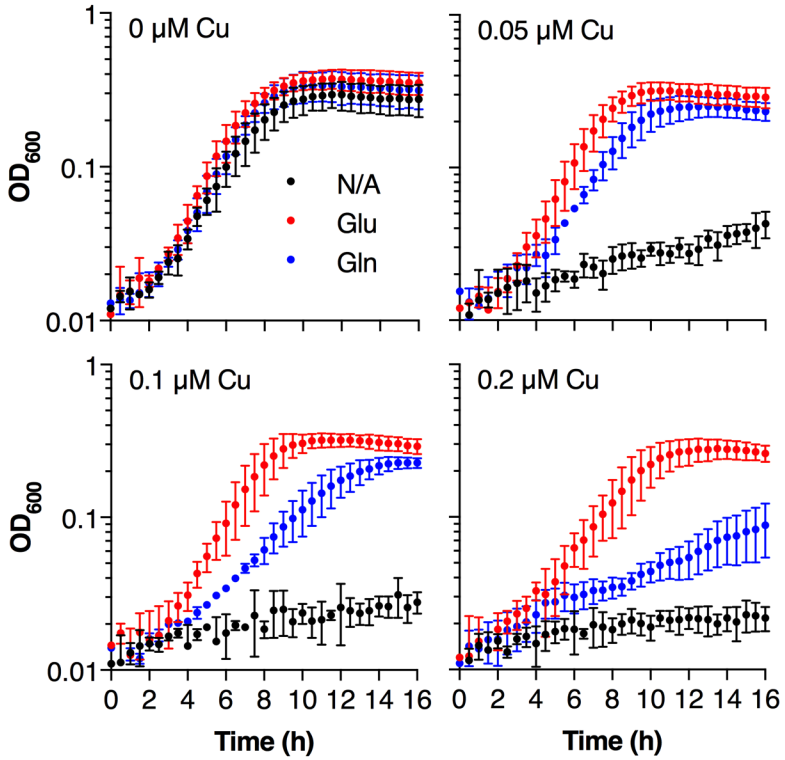

Figure S8. Separate protective effects of Glu and Gln. *E. coli* UTI89Δ*copA* mutant strain was grown at pH 5 in the presence of 0 – 0.2 μM added Cu. The culture medium was supplemented with water (black), 0.5 mM Glu (red), or 0.5 mM Gln (blue). Data were averaged from three independent experiments. Error bars represent ± SD.

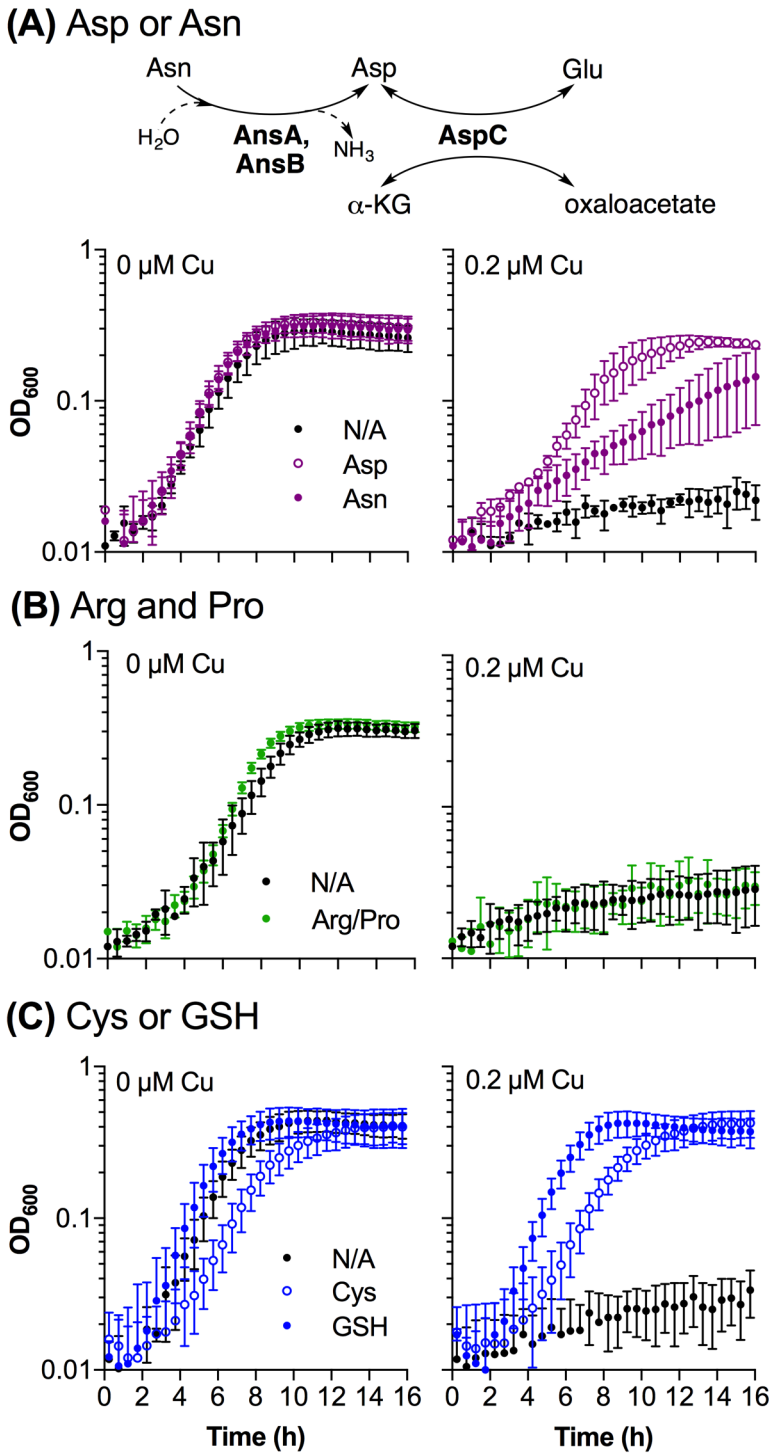

Figure S9. Protective effects of (A) Asp or Asn, (B) Arg and Pro, (C) Cys or GSH. *E. coli* UTI89Δ*copA* mutant strain was cultured at pH 5 in the presence of 0 or 0.2 μM added Cu. The medium was supplemented with water (N/A, black circles) or 0.5 mM of each amino acid as indicated. Data were averaged from three independent experiments. Error bars represent ± SD. Pathway for the generation of Glu from Asn and Asp *via* the two asparaginases in *E. coli* (AnsA and AnsB) and aspartate aminotransferase (AspC) was shown in panel (A).

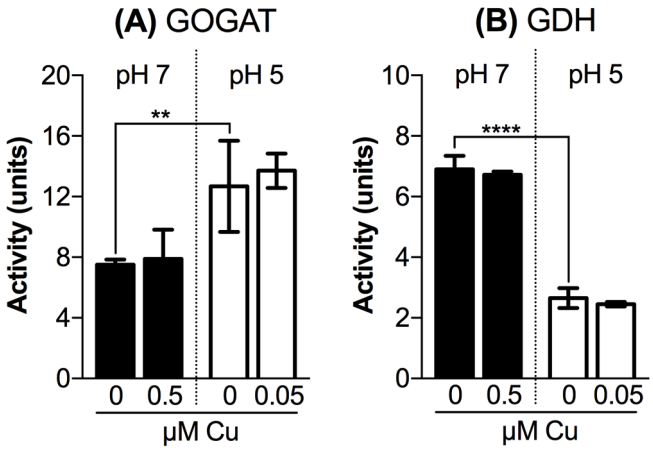

Figure S10. Effects of Cu on the activities of glutamate-synthesising enzymes in WT bacteria. UTI89 WT was cultured at pH 7 (black columns) in the presence of 0 or 0.5 µM Cu, or at pH 5 (white columns)in the presence of 0 or 0.05 µM Cu. Mid-exponential cells were collected and activities of **(A)** GOGAT and **(B)** GDH were measured in cell-free lysis extracts. Data were averaged from three independent experiments. Error bars represent ± SD. GOGAT activities were reproducibly higher in bacteria cultured at pH 5 ($^{**}P < 0.01$) while GDH activities were higher in bacteria cultured at pH 7 ($^{****}P < 0.0001$).

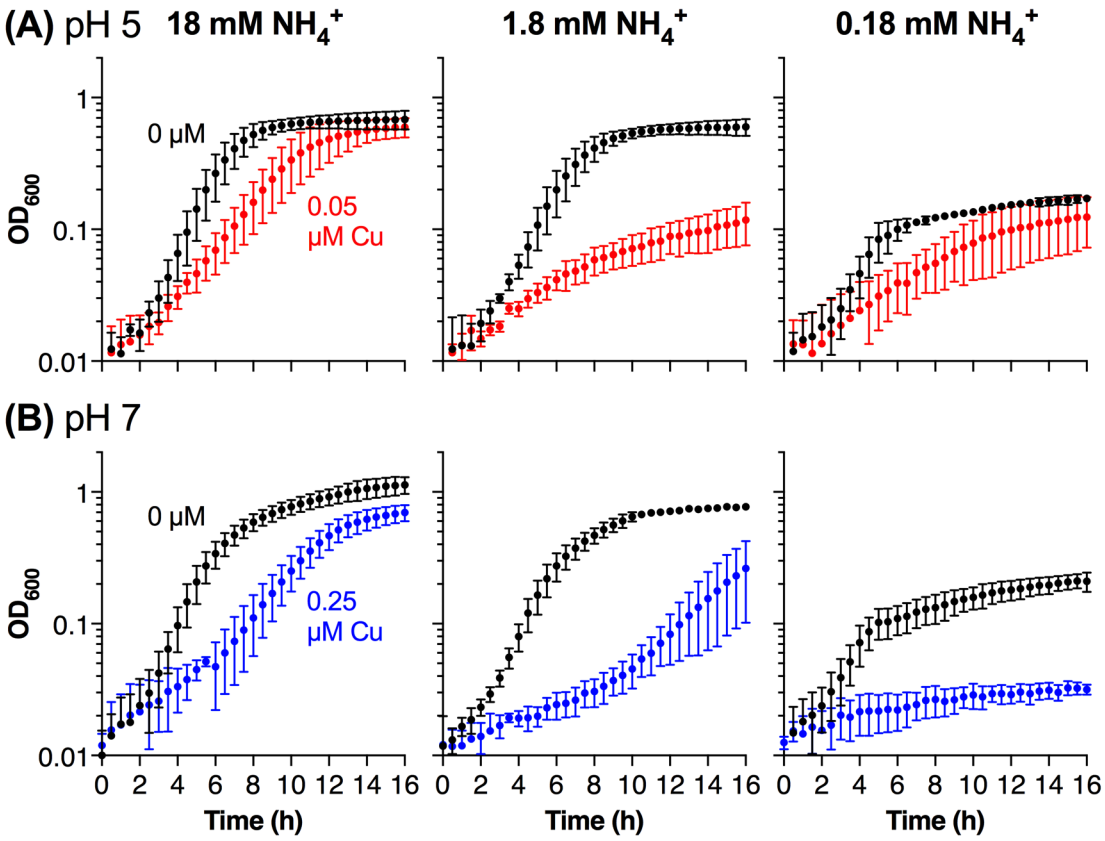

Figure S11. Effects of ammonia availability on Cu stress. *E. coli* UTI89Δ*copA* mutant strain was grown at **(A)** pH 5 or **(B)** pH 7 with or without Cu as indicated. The culture medium contained 18, 1.8, or 0.18 mM ammonium chloride as the sole nitrogen source. Data were averaged from four independent experiments. Error bars represent ± SD.

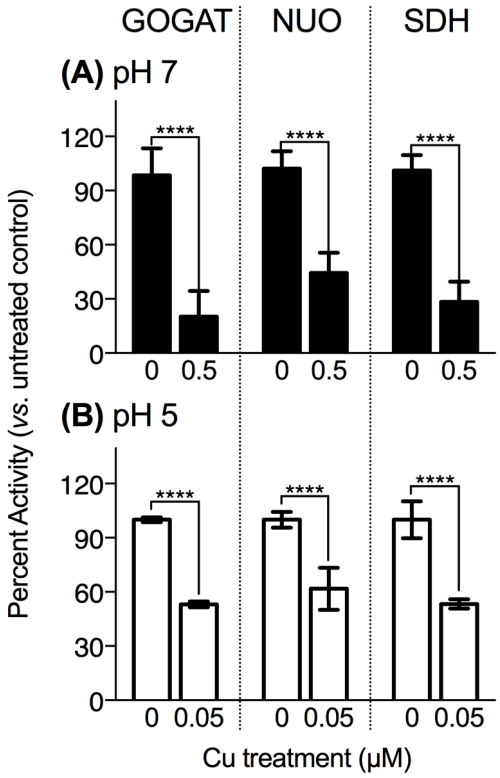

Figure S12. Effects of Cu on the activities of iron-sulfur enzymes. *E. coli* UTI89Δ*copA* mutant strain was cultured **(A)** at pH 7 in the presence of 0 or 0.5 μM added Cu or **(B)** at pH 5 in the presence of 0 or 0.05 μM added Cu. Mid-exponential cells were collected and activities of GOGAT, NUO, and SDH were measured in cell-free lysis extracts. Results were normalised to the untreated control (cultured with 0 μM added Cu). Data were averaged from three independent experiments. Error bars represent ± SD. $^{****}P < 0.0001$.

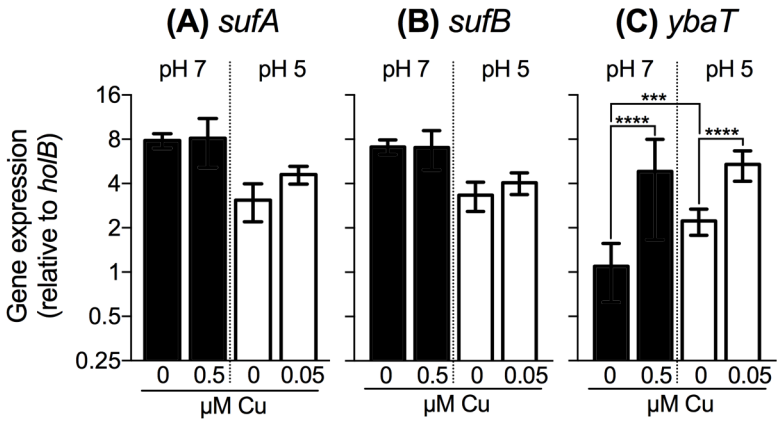

Figure S13. Effects of Cu on expression of (A) *sufA*, (B) *sufB*, and (C) *ybaT*. *E. coli* UTI89Δ*copA* mutant strain was cultured at pH 7 (black columns) or in the presence of 0 or 0.5 µM Cu at pH 5 (white columns) in the presence of 0 or 0.05 µM Cu. Total RNA was extracted from mid-exponential cells and amounts of transcripts relative to *holB* were measured by qPCR. Data were averaged from six independent experiments. Error bars represent ± SD from the mean. $^{***}P < 0.001$, $^{****}P < 0.0001$.

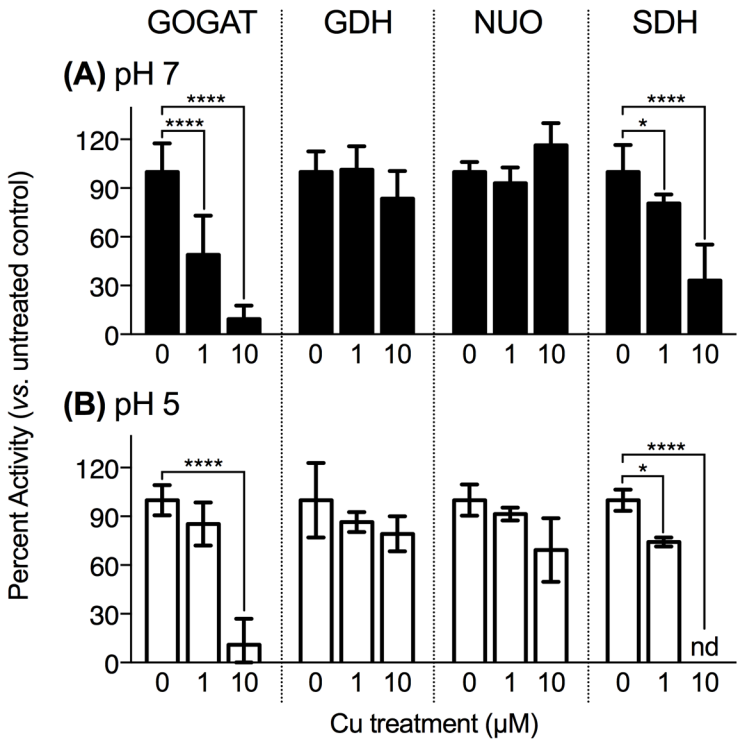

Figure S14. Excess Cu ions may directly damage GOGAT. *E. coli* UTI89Δ*copA* mutant strain was cultured at **(A)** pH 7 or **(B)** pH 5 without any added Cu to the mid-exponential phase and was subsequently challenged with 0, 1, or 10 μM Cu. After 30 min, cells were collected and activities of GOGAT, GDH, NUO, and SDH were measured in cell-free lysis extracts. Data were averaged from three independent experiments. Error bars represent ± SD. $^{****}P < 0.0001$, $^{*}P < 0.05$.

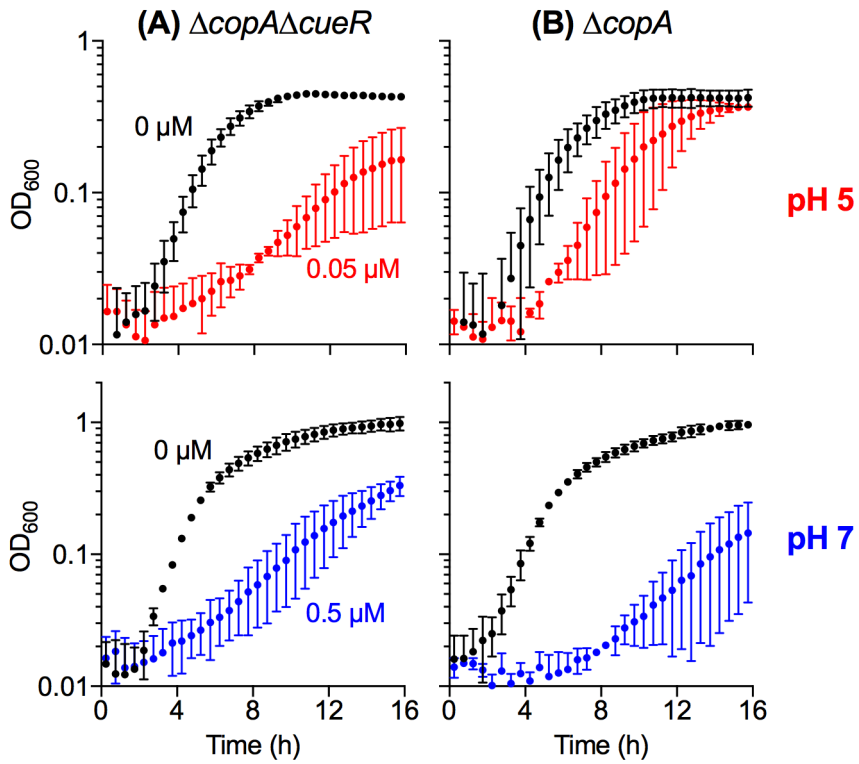

Figure S15. Cu stress in the UTI89Δ*copA*Δ*cueR* mutant. Bacteria were cultured at pH 5 in the presence of 0 or 0.05 μM of added Cu (top panels) or at pH 7 in the presence of 0 or 0.5 μM of added Cu (bottom panels). Data were averaged from three independent experiments. Error bars represent ± SD. Cu stress in the UTI89Δ*copA* parent mutant was assessed in parallel and the results were shown for comparison.

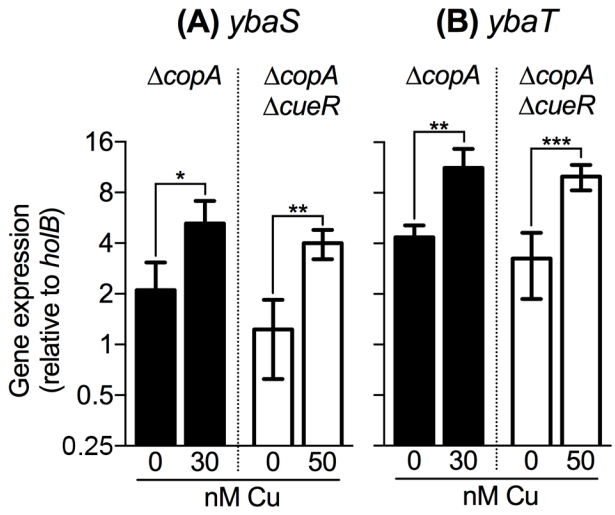

Figure S16. Effects of Cu on expression of (A) *ybaS* and (B) *ybaT* in the UTI89Δ*copA*Δ*cueR* mutant. Bacteria were cultured at pH 5 in the presence of 0, 30, or 50 nM of added Cu as indicated. Data were averaged from three independent experiments. Error bars represent ± SD. $^{*}P < 0.05$, $^{**}P < 0.01$, $^{***}P < 0.001$. Results from parallel experimentation with the UTI89Δ*copA* parent mutant strain were shown for comparison.

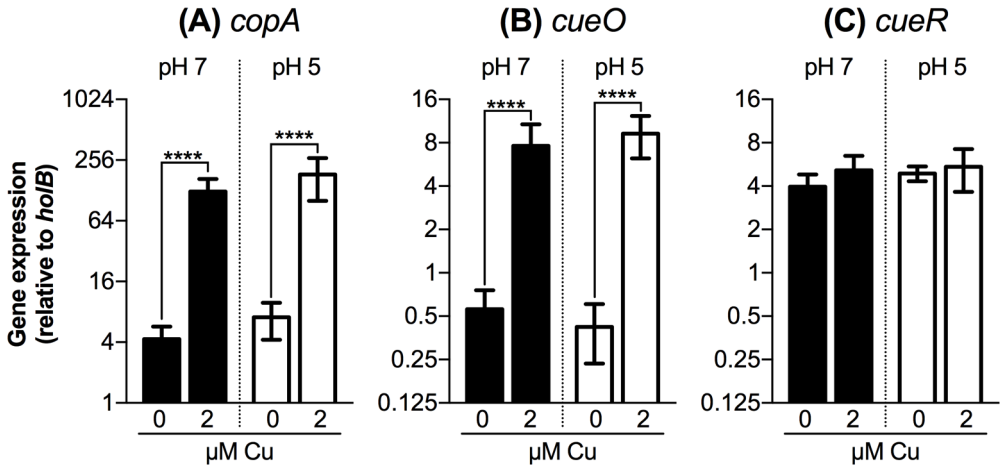

Figure S17. Effects of pH on the expression of Cu tolerance genes in WT cells. The UTI89 WT strain was cultured at pH 7 (black columns) or pH 5 (white columns) in the presence of 0 or 2 µM Cu. Total RNA was extracted from mid-exponential cells and amounts of **(A)** *copA*, **(B)** *cueO*, and **(C)** *cueR* transcripts relative to *holB* were measured by qPCR. Data were averaged from six independent experiments. Error bars represent ± SD from the mean. $^{****}P < 0.0001$.

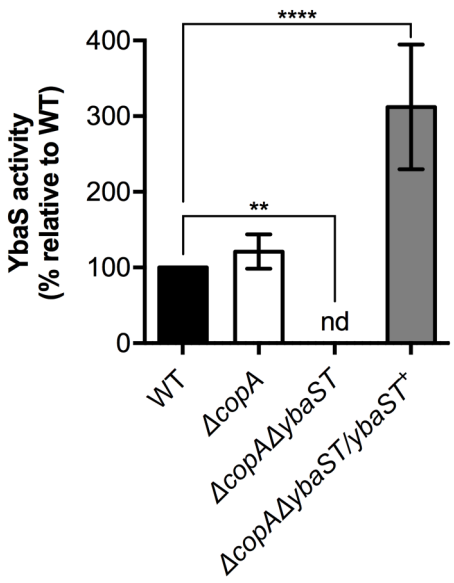

Figure S18. YbaS activity in Δ*ybaST* mutant strains. Bacteria were propagated on Cu-free LB agar overnight and cells from the agar plate were harvested and lysed. YbaS activities were measured in cell-free lysis extracts. Results were normalised to the WT. Data were averaged from three independent experiments. Error bars represent ± SD. nd, not detectable (below detection limit). $^{****}P < 0.0001$, $^{**}P < 0.01$.

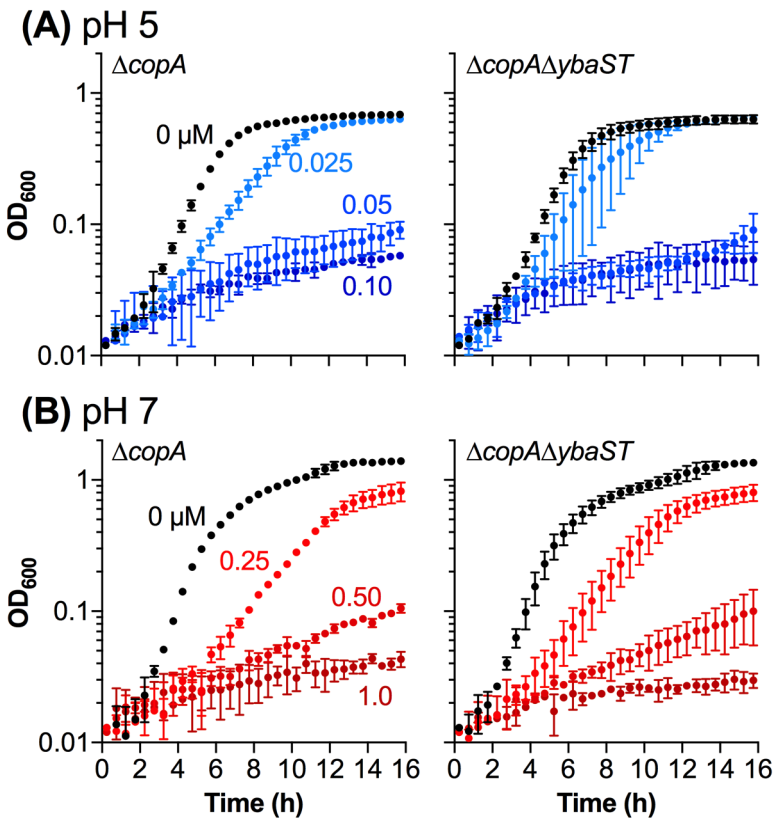

Figure S19. Cu stress in the Δ*copA*Δ*ybaST* mutant strain. Growth of EC958Δ*copA* and Δ*copA*Δ*ybaST* mutant strains **(A)** at pH 5 in the presence of 0 – 0.10 µM of added Cu and **(B)** at pH 7 in the presence of 0 – 1.0 µM of added Cu. Data were averaged from three independent experiments. Error bars represent ± SD.

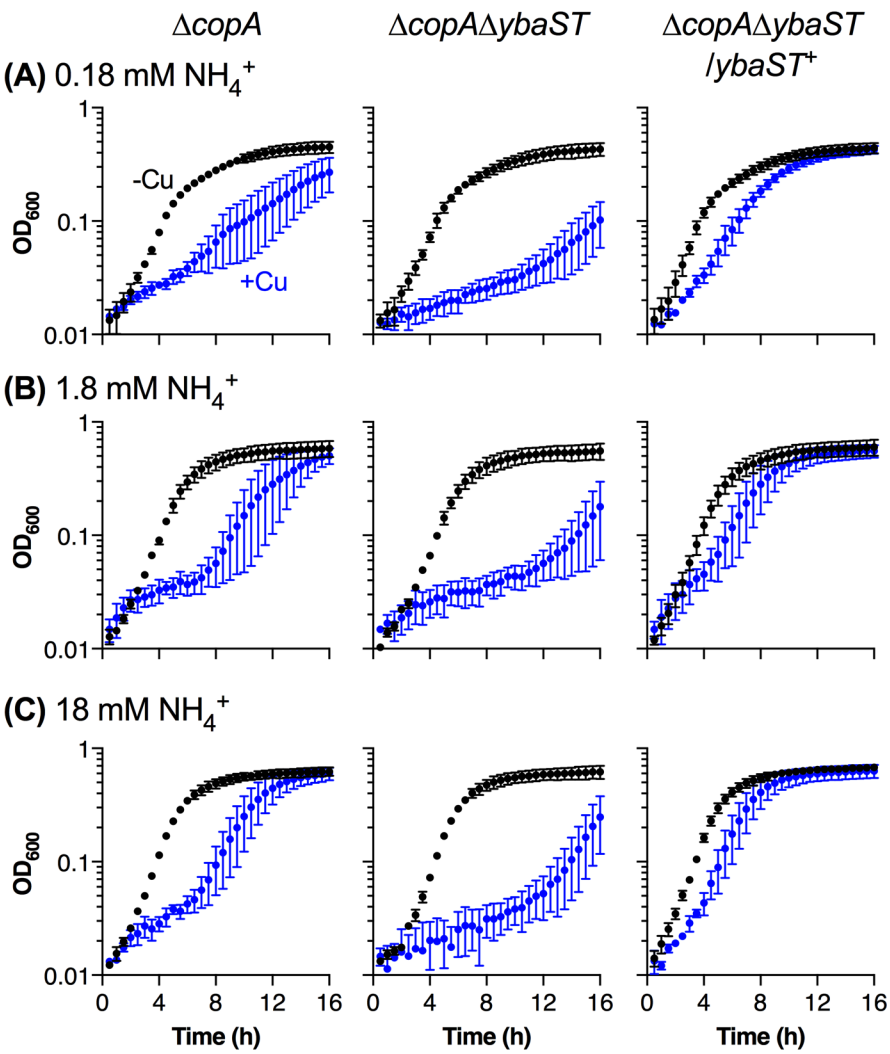

Figure S20. Effects of ammonia availability on Cu stress in the Δ*copA*Δ*ybaST* mutant. *E. coli* EC958 Δ*copA* mutant, Δ*copA*Δ*ybaST* double mutant, and Δ*copA*Δ*ybaST*/*ybaST*$^{+}$ complemented mutant strain was cultured at pH 5 with 0 (-Cu, black traces) or 0.05 µM of added Cu (+Cu, blue traces). The culture medium contained 0.5 mM Gln and **(A)** 0.18, **(B)** 1.8, or **(C)** 18 mM ammonium chloride. Data were averaged from three independent experiments. Error bars represent ± SD.